



Cite this: *J. Anal. At. Spectrom.*, 2024, 39, 1600

In-line HPLC-ICP-MS method for the rapid speciation and quantification of metal constituents in cell culture media

Cameron J. Stouffer, Sarah K. Wysor and R. Kenneth Marcus *

It is well established that the metal content in Chinese hamster ovary (CHO) cell culture media (CCM) greatly affects process productivity and critical quality attributes (CQAs). Metals exist in diverse chemical forms in CCM, which may change during the monoclonal antibody (mAb) production cycle. Naturally, it is postulated that the chemical speciation of these metals affects their uptake and metabolism. While the targeted forms of metals in media are company-specified, their commercial sources, as well as those of the organic media constituents, may result in concentrations and speciation that differ from the intended formulae. Therefore, there is a need for a method to determine the concentration of metals and their chemical forms. Presented here is a methodology to speciate inorganic-versus-ligated metals using high-performance liquid chromatography (HPLC) employing a polypropylene capillary-channeled (C-CP) fiber column with inductively coupled plasma mass spectrometry (ICP-MS) determinations of five target metals (Mn, Fe, Co, Cu, and Zn). A 50 μ L injection of CCM supernatant is used for an effective quantification method to identify metal speciation and concentration deviations from reported formula levels. Two case studies as to the utility of the methodology are presented: potential chemical contamination and species variability due to shelf-life. Further development of this method has relevance towards quality control, identification of contaminants, assessment of media stability/degradation products, and measurement of whole cell metal uptake in growth media.

Received 8th February 2024

Accepted 30th April 2024

DOI: 10.1039/d4ja00049h

rsc.li/jaas

1. Introduction

The culturing of Chinese hamster ovary (CHO) cells in cell culture media (CCM) is a prominent process for the production of biotherapeutics, especially monoclonal antibodies (mAbs) such as immunoglobulin G (IgG).^{1–6} Investigations into the media's productivity and critical quality attributes (CQAs) have established metal content as a main effector of CCM efficacy.^{6,7} The bioavailability of the metal components in media is crucial to their effectiveness; too little and the cells cannot be adequately nourished, while too much can lead to cellular toxicity, potentially killing the cells.^{6,8–12} While it is known that levels of metal content affect the cells' ability to grow in CCM,^{6,13–17} little is known about the speciation of the metals in CCM and how their chemical form affects cellular growth and uptake. It is postulated that these metals may change form in CCM and throughout the cell growth process due to cellular metabolism, ultimately affecting the cellular growth and uptake of these metals. As such, the composition of the media, and how that composition changes over time, is of the utmost concern to researchers and pharmaceutical manufacturers.

For the culturing of cells, growth media, which typically contains amino acids, carbohydrates, inorganic (metal) salts, and other biologically beneficial species, is used. Basal media, the initiating growth media, is primarily composed of amino acids, carbohydrates, inorganic salts, vitamins, and other nutrients.¹⁸ As many transition metals, such as cobalt, copper, and iron, act as the active centers of many essential enzymes and coenzymes, they are added into CCM to support cellular processes.^{6,12,18} However, variations in CCM metal composition from the targeted formula have been reported with variations present from batch to batch.^{1,6,8,12,17–20} Unintentional variations in metal content are thought to be caused by contamination from the input chemicals (e.g., amino acids) used in the CCM formulation. This results in higher concentrations of metals that can affect cell culture outcomes, alter the pH, osmolarity, and generally introducing variability in the production results; commonly known as critical quality attributes (CQAs).^{6,8,17,18,21–26} While variations in total metals content would seem to have obvious implications in culture productivity, a more subtle, yet potentially more impactful set of variables involves the chemical speciation of those metals.

Despite specific implications of metal speciation only now becoming the topic of study, it is not hard to imagine that the chemical form of a metal (inorganic ion, types of ligands, etc.) will have a bearing on the uptake of the metal into the host cells



as well as how they are metabolized internally.¹² For example, inorganic Fe^{2+} and Cu^+ have the potential to generate reactive oxygen species (ROS) through redox reactions. Elevated levels of ROS can create oxidative stress leading to cellular damage, DNA damage, and disruption of cellular functions, as well as impact cell viability, proliferation, and overall cell health.^{27–29} Imbalance in metal content can also indirectly affect cells by interacting with proteins present in cell culture media essential for growth. These interactions can affect protein folding, stability, and activity. For instance, low levels of Cu^{2+} can prevent the metabolic lactate shift, hindering cell growth, whereas a high level of Cu^{2+} can lead to high levels of proteins.^{30–32} This can impact cellular signaling pathways, enzyme activity, and overall cell function.¹² Additionally, some CCM supplements, such as fetal bovine serum (FBS), may contain natural metal-binding proteins or chelators, which must be accounted for.³³ These proteins and other small molecule chelators, such as amino acids, can sequester or bind metals present in the media, altering their intended form, and perhaps negating the positive aspects of these metals in media, producing a need for metal speciation identification and quantification.

As the chemical form of metals are postulated to have similar effects as metal concentrations on CCM efficacy fundamental questions, such as most preferred forms for cellular uptake/metabolism, potential changes of speciation in-process, and the like are unanswered. To explore this, it is imperative to develop analytical methods capable of separating and quantifying differences in both speciation and concentration of available supplemental nutrients. Presented here is a rapid method for the in-line species characterization (inorganic vs. ligated)³⁴ and quantification of five metals (Mn, Fe, Co, Cu, & Zn) common to CCMs, utilizing a standard high performance liquid chromatography (HPLC) platform coupled to inductively coupled mass spectrometry (ICP-MS). The separations of inorganic and ligated species were performed using trilobal polypropylene (PPY) capillary-channeled polymer (C-CP) fibers as a stationary phase for a reversed phase solid phase extraction (SPE) process, as previously described.^{35,36} The inorganic ions and ligated species were then analyzed with ICP-MS, following a post column dilution, to determine the respective quantity and speciation states of the metals. This method provides a rapid determination of the speciation of the target metals in the media, potentially providing insights into the sources of contamination of the metals in the media processing and changes to their speciation states throughout production.

2. Methods and materials

2.1 Sample preparation

Solutions of inorganic Mn, Fe, Co, Cu, and Zn (High Purity Standards (HPC), North Charleston, SC) were purchased in stocks of 1000 mg mL^{-1} . Solutions of each analyte were made in concentrations $\sim 100 \times$ above and below their reported formula concentrations in AMBIC 1.1 (Advance Mammalian Bio-manufacturing Innovation Center) CCM,³⁷ (Mn: 5.0×10^{-8} to 5.0×10^{-4} mM, Fe: 1.0×10^{-3} to 1.0×10^1 mM, Co: 1.0×10^{-5} to 1.0×10^{-1} mM, Cu: 1.0×10^{-6} to 1.0×10^{-2} mM, Zn: 1.0×10^{-4}

to 1.0×10^0 mM). Solutions were made in ultra-pure 2% nitric acid made from concentrated (70%) ultra-pure nitric acid (VWR Chemicals, Radnor, PA) and Aristar ultra-pure water (VWR Chemicals, Radnor, PA). A standard solution of the inorganic and ligated forms of the five target metals was made according to the published formulation, using manganese chloride (MnCl_2 , Acros Organics, Thermo Scientific, NJ), ferric ammonium citrate ($\text{C}_6\text{H}_8\text{O}_7 \cdot x\text{Fe}_3^+ \cdot y\text{NH}_3$, Sigma Aldrich, St. Louis, MO), cyanocobalamin (VB_{12} , Spectrum Chemical Mfg. Corp., New Brunswick, NJ), cupric sulfate (CuSO_4 , Fisher Scientific, Hampton, NH), and zinc chloride (ZnCl_2 , VWR Chemicals, Radnor, PA). The five target metallic forms were added in concentrations they are present in formulated media (5.05×10^{-6} mM, 0.133 mM, 0.003 mM, 2.69×10^{-4} mM, and 0.014 mM for Mn, Fe, Co, Cu, and Zn, respectively).³⁷ All samples were then placed on an Analog Vortex Mixer (VWR International, Radnor, PA) and vortexed for 60 seconds to ensure the metals were completely dissolved in the water. Basal CCM samples were purchased from Sigma-Millipore (St. Louis, MO).

2.2 In-line HPLC-ICP-MS components and methods

Reversed phase (RP) separations were performed using a Thermo Fisher Ultimate 3000 HPLC unit, consisting of a quaternary pumping system and injector (the standard absorbance unit was not employed). A microbore polypropylene (PPY) C-CP fiber column, assembled in this laboratory from fibers extruded in the Department of Materials Science at Clemson University,³⁸ was mounted in place of the standard commercial column. The tri-lobal fibers (~ 630 fibers) were pulled through 30 cm of polyether ether ketone (PEEK) tubing (0.78 mm i.d.) (Cole-Palmer, Vernon Hills, IL, USA). The fiber column was used to separate the inorganic ions (unretained) and ligated species (retained) of CCM using a reversed-phase protocol as previously described,^{35,39} wherein the free metal ions pass through the column directly to the plasma and the ligated species are subsequently eluted using an 80 : 20 ACN : H_2O mixture.

The coupling of the HPLC separation platform to the ICP-MS is illustrated in Fig. 1. Briefly, test solutions were injected (50 μL) onto the PPY C-CP fiber column in ultra-pure (UP)- H_2O + 0.1% TFA at a flow rate of $500 \mu\text{L min}^{-1}$. A solvent gradient step to 80% ACN + 0.1% TFA was then initiated at $t = 4$ min following the initial injection to elute the adsorbed, ligated species from the column (depicted in Fig. 2). Following passage through the column, the solutions (the native injection matrix and the ACN : H_2O eluates) were split 1 : 10 and the flow subsequently supplemented back to $500 \mu\text{L min}^{-1}$ with 2% HNO_3 (effectively a 10% dilution) and carried to the nebulizer for ionization and quantification by ICP-MS. Use of the nitric acid matrix allows for ready quantification using the same standard response curves for both elution matrices as well as serve to dilute the ACN content down to 8% to assure stable plasma operation. The HPLC was coupled to the Solion ICP-MS (Advion Corp., Ithaca, NY, USA) via a MicroFlow PFA nebulizer (NexION2000, ESI, Omaha, NE) housed within a custom quartz cyclonic spray chamber (ESI, Omaha, NE). The ICP-MS operating conditions are presented in Table 1. The individual transient elemental



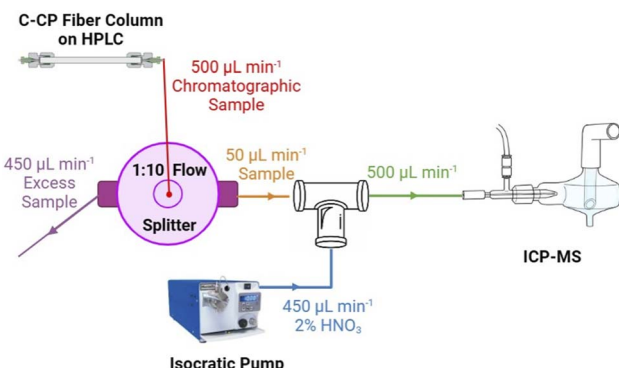


Fig. 1 Illustration of HPLC employing a polypropylene C-CP fiber column and ICP-MS for in-line differentiation and quantification of metals in cell culture media. A 1 : 10 flow splitter and merging *t*-fitting is used in combination to affect a 1 : 10 dilution of the respective carrier solvents for matrix normalization and suitability for introduction in the ICP plasma.

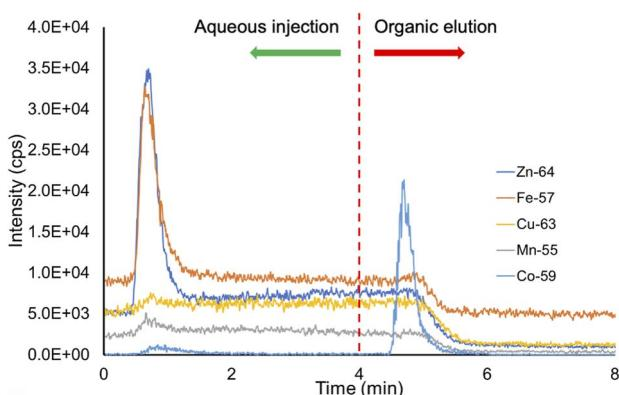


Fig. 2 Demonstrative temporal profiles of C-CP fiber separation and ICP-MS detection of inorganic and ligated species. Initial peaks represent the non-retention of the inorganic species and direct passage to the plasma, with the organic solvent (80 : 20 ACN : H₂O) introduction initiated at *t* = 4 min.

Table 1 Solation ICP-MS operation conditions

Parameter	Unit	Value
Plasma gas flow rate	L min ⁻¹	16.0
Auxiliary gas flow rate	L min ⁻¹	0.8
Carrier gas flow rate	L min ⁻¹	1.30
Peristaltic pump rate	rpm	30
RF power	W	1400
Sampling depth	mm	4.0
Einzel lens 1	V	-8
Einzel lens 2	V	-48
Octapole exit	V	-20
Octapole bias	V	-22
Collisional gas flow rate	L min ⁻¹	0

signal responses were integrated in the newly-updated Advion Data Express for ICP-MS software using the “Process List for Quantitation” peak integration function. While it will be

discussed in detail in subsequent sections, Fig. 2 illustrates a typical ICP-MS signal output, illustrating the direct transit of inorganic species to the plasma yielding ICP-MS transient responses at time = ~0.5 min, with the ACN : H₂O wash initiated at time = 4 min, eluting the bound, ligated species. The analyte signals for the respective elution bands were integrated for a total time of 60 seconds, with the elution time set to the center of the signal transient of each sequence.

3. Results and discussion

3.1 Matrix considerations for in-line ICP-MS analysis

The speciation of metals using the polypropylene C-CP fiber column utilizes a reversed-phase separation method, where organic solvents are used for the elution of retained ligated species.^{35,36} In a standard analysis using ICP-MS, a solution containing 1–5% HNO₃ is typically used as the carrier solution. The addition of organics to the carrier solution can have minimal positive effects, including the reduction of ionization instabilities and spatial/temporal fluctuations in the plasma and the enhancement of the ionization efficiency of certain elements.⁴⁰ Despite potential benefits, the addition of organic constituents into the ICP often causes severe effects and changes in the plasma's thermal properties, leading to variations in the ionization efficiency and background noise. It can also cause changes in the volatility of the sample matrix, which might cause a decrease in the sample transport efficiency, and changes to the nebulization efficiency, altering droplet size and aerosol characteristics, impacting the overall sensitivity and accuracy of the analysis. Finally, introduction of organic solvents has the particularly deleterious effect of depositing soot on the sampling cone, effecting the conductivity of the cone, leading to severe instability and potential clogging.^{41–47} As such, many different approaches to mitigate the effects of organic solvents have been developed, including optimization of ICP operating conditions including sample introduction rate, carrier gas flow rate, RF power, *etc.*, the reduction of carbon concentration introduced into the plasma, change to mobile phase pH, timing of separation gradient changes, *etc.*^{41,46,48,49} Given that organic-phase elution is required, the effect of the elution mobile phase on ICP stability, ionization efficiency, and spectral effects needs to be explored.

To assess the potential effects of the organic matrices on the responses of the five target metals, a 1 : 10 dilution of 80% ACN + 0.1% TFA (ligated species elution step) followed with 2% HNO₃ was performed. Linearity of responses for the relevant concentrations of ⁵⁵Mn and ⁶³Cu in CCM can be seen in Fig. 3. A summary for each of the five analyte's response functions, *R*², LOD, and LOQ, for analysis in a standard 2% HNO₃ solution and the 1 : 10 dilution of the ligated-species elution step matrix with 2% HNO₃ is found in Table 2. The addition of the organic constituents in the matrix was seen to have no significant effect on the ICP-MS responses for any of the five analytes as they all produced similar sensitivity, detection limits, and linearity in both the aqueous 2% HNO₃ matrix and the 1 : 10 80% ACN + 0.1% TFA: 2% HNO₃ matrix. It can be concluded that a 1 : 10 dilution using 2% HNO₃ is sufficient to mitigate any potential



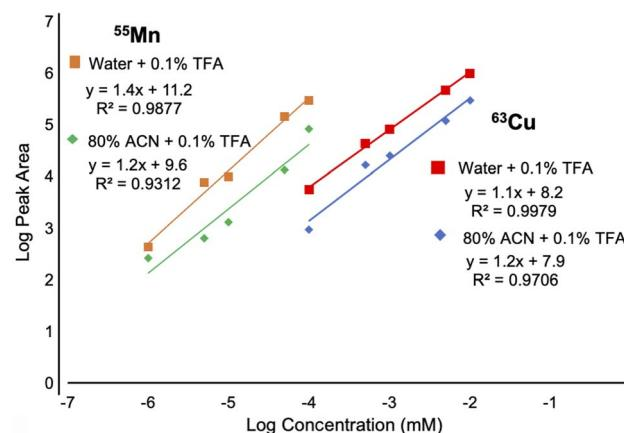


Fig. 3 Demonstrative response curves for ^{55}Mn and ^{63}Cu using the flow splitter and *T*-fitting apparatus, confirming quantitative recoveries.

deleterious effects inflicted by the organic solvent. Stated another way, the Solation ICP-MS is robust towards the introduction of as much as 8% ACN in the carrier solvent.

Beyond the results for the inorganic metals of Table 2, it was necessary to confirm that the ionization efficiencies of cobalt in both the VB_{12} and CoCl_2 forms were not different, *i.e.*, no species bias. Therefore, the response of Co in the two forms was compared. Solutions were made from 1.0×10^{-5} mM to 1.0×10^{-1} mM in the two plasma introduction matrices; 1 : 10 H_2O + 0.1% TFA: 2% HNO_3 and 1 : 10 80% ACN + 0.1% TFA: 2% HNO_3 . In the aqueous matrix, CoCl_2 and VB_{12} produced responses with logarithmic slopes of 0.9133 and 0.9319, with R^2 values of 0.9984 and 0.9746, respectively. When introduced in the organic matrix, CoCl_2 and VB_{12} responded in a similar fashion with logarithmic slopes 0.9354 and 0.9194, and R^2 values of 0.9974 and 0.9972, respectively. These responses reveal no appreciable differences in their ionization characteristics based on chemical speciation, in either matrix.

3.2 Integration of HPLC to ICP-MS

As discussed before, addition of organics to the matrix affects plasma stability, but it was found that a 1 : 10 dilution with 2%

HNO_3 was sufficient to relieve any negative effects of the separation matrix to the plasma's ability to ionize the five target analytes. To make a fully integrated in-line separation and detection method using the HPLC and ICP-MS system, a dilution step needs to be added to reduce the organic matrix from the separation. For this aim, an apparatus using a 1 : 10 flow splitter and a *T*-fitting for a 1 : 10 dilution was constructed, as illustrated in Fig. 1. Responses of the five target analytes (^{55}Mn , ^{57}Fe , ^{59}Co , ^{63}Cu , and ^{64}Zn) were analyzed from at a concentration 100 \times above and below their reported product formula concentration. Responses were evaluated by the peak transient values of triplicate measurements, with the analytical figures of merit presented in Table 3. All five analytes produced linear responses in both matrices when injected onto the column and carried through the entire analytical protocol. These responses confirmed the stable and reproducible flow splitting, dilution, and ionization processing of the five analytes using the integrated HPLC and ICP-MS system.

3.3 Separation of inorganic and ligated species

CCM contains a plethora of metal compounds to be used as supplements for various cellular processes. These metals ultimately help to sustain and support cell life and growth; however, both the concentration and speciation of these metals often deviate from the intended product formula. Indeed, the concentrations and speciation states may change in the course of the culture process. The five common metal supplements used in the AMBIC 1.1 CCM include Mn, Fe, Cu, and Zn, which are added as inorganic metal species, whereas Co is added as vitamin B₁₂ (VB_{12}), a Co-complexed vitamin. According to the published formula, the input concentrations are: 5.05×10^{-6} mM of ferric ammonium citrate, 0.133 mM of manganous chloride, 0.003 mM of VB_{12} , 2.69×10^{-4} mM of zinc chloride, and 0.014 mM of cupric sulfate.³⁷

To this extent, the in-line speciation and detection of metal species in CCM using the integrated HPLC-ICP-MS system was tested for accuracy using an in-house prepared mixture of the species in aqueous solution for use as a standard *versus* the supplied AMBIC media. Calibration functions were generated for the analytes across concentrations of 0.01 to 100 \times the formula values. Fig. 2 illustrates a typical separation sequence

Table 2 ICP-MS analytical response functions and figures of merit for the inorganic test elements in 2% HNO_3 (acid) and the organic elution solvent (80 : 20 ACN : H_2O) diluted 1 : 10 in 2% HNO_3

Element/isotope	Carrier solvent	Response function (log-log)	R ²	LOD (pg mL ⁻¹)	LOQ (pg mL ⁻¹)
^{55}Mn	2% HNO_3	$y = 0.93x + 0.87$	0.9985	1.3	4.2
	1 : 10 organic : acid	$y = 0.87x + 1.45$	0.9942	1.3	4.3
^{57}Fe	2% HNO_3	$y = 0.96x - 0.62$	0.9999	1.2	3.9
	1 : 10 organic : acid	$y = 0.90x - 0.05$	0.9961	1.3	4.2
^{59}Co	2% HNO_3	$y = 0.96x + 1.25$	0.9989	1.9	6.2
	1 : 10 organic : acid	$y = 0.92x + 1.66$	0.9972	1.3	4.2
^{63}Cu	2% HNO_3	$y = 0.92x + 1.38$	0.9974	1.2	4.0
	1 : 10 organic : acid	$y = 0.94x + 0.60$	0.9975	1.2	3.9
^{64}Zn	2% HNO_3	$y = 0.92x + 0.60$	0.9998	1.2	4.0
	1 : 10 organic : acid	$y = 0.94x - 0.09$	0.9950	1.1	3.5



Table 3 ICP-MS analytical response functions and figures of merit for test elements in the aqueous (water + 0.1% TFA) and organic (80 : 20 ACN : H₂O) elution solvents, followed by the 1 : 10 flow split and 10× dilution with 2% HNO₃

Element/isotope	Carrier solvent	Response function (log-log)	R ²	LOD (pg mL ⁻¹)	LOQ (pg mL ⁻¹)
⁵⁵ Mn	Water + 0.1% TFA	$y = 1.4x + 11.2$	0.9877	4.7	16
	80% ACN + 0.1% TFA	$y = 1.2x + 9.6$	0.9312	10	33
⁵⁷ Fe	Water + 0.1% TFA	$y = 1.3x + 6.6$	0.9627	2.6×10^4	8.9×10^4
	80% ACN + 0.1% TFA	$y = 1.2x + 6.0$	0.9828	1.4×10^4	4.7×10^4
⁵⁹ Co	Water + 0.1% TFA	$y = 1.1x + 8.6$	0.9840	65	2.2×10^2
	80% ACN + 0.1% TFA	$y = 1.2x + 8.0$	0.9819	98	3.3×10^2
⁶³ Cu	Water + 0.1% TFA	$y = 1.1x + 8.2$	0.9979	8.0×10^2	2.7×10^3
	80% ACN + 0.1% TFA	$y = 1.2x + 7.9$	0.9706	8.4×10^2	2.8×10^3
⁶⁴ Zn	Water + 0.1% TFA	$y = 0.9x + 7.6$	0.9913	1.3×10^3	4.1×10^3
	80% ACN + 0.1% TFA	$Y = 1.0x + 7.1$	0.9858	2.6×10^3	8.6×10^3

for an AMBIC media sample, where the metals introduced as salts all show responses corresponding to the injection band, while Co shows some small response with that group and a more prominent band observed with the organic eluate. The experimentally determined concentrations and percentage recoveries of triplicate measurements for the five target metals can be seen in Table 4. The percentage recoveries for the inorganic metals ranged from 92.9% to 105.0%. The appearance of Co in both fractions is evidence of some dissociation of the metal from the core of the vitamin; as had been seen previously with this analyte.³⁹ Interestingly, the fraction of the free Co, 10.4% dissociated, compares directly to fundamental studies of VB₁₂ equilibria measurements during photolytic reactions where 10% of the cobalt was observed to dissociate,⁵⁰ with the composite concentration of the inorganic and ligated Co yielded a recovery of 95.7%. As seen in Table 4, the precision of the method also shows excellent reproducibility with all elements having standard deviations ten percent or less relative to the calculated value. The evaluation of the standard solution through the complete analytical method proved the method to be quantitatively accurate, with analytical percent recoveries.

3.4 Case study 1: process media analysis and potential metal contamination

As described previously, there can often be differences among the actual metal content between lots prepared according to the 'same formula'. It is typical in this industry to prepare media from gravimetrically portioned dry components, with dissolution in H₂O. Deviations from expected concentrations/species

can be due to the weighing process, contamination brought in by other components, or the water system. Fig. 4 is a photograph of 3 AMBIC 1.1 basal medial bottles (lot numbers provided in caption) that should have the same metal content and speciation, with the only difference being that Basal 3 contains no glucose. It is visually clear that while Basal 1 and 3 are very similar, Basal 2 has a different hue; golden rather than



Fig. 4 Photograph of bottles of AMBIC CCM basal media. From left to right: Basal 1 – Lot. No. 22G015 (DOM July 18th, 2022), Basal 2 – 22L270 (DOM November 18th, 2022), and Basal 3 – 22L271 (DOM November 21st, 2022).

Table 4 Comparison of experimentally determined concentrations to the commercial media formula composition of a mixed species solution for method testing of the integrated HPLC-ICP-MS

Species	Formula concentration (mM)	Experimental concentration (mM)	%Recovery	Total %recovery
Inorganic – Mn	5.05×10^{-6}	$5.1 \times 10^{-6} \pm 5.0 \times 10^{-7}$	101.8	
Inorganic – Fe	1.33×10^{-1}	$1.3 \times 10^{-1} \pm 7.6 \times 10^{-3}$	98.7	
Inorganic – Co	0	$2.7 \times 10^{-4} \pm 1.2 \times 10^{-5}$	n/a	95.7
Ligated – Co	3.0×10^{-3}	$2.6 \times 10^{-3} \pm 8.5 \times 10^{-5}$	86.7	
Inorganic – Cu	2.69×10^{-4}	$2.5 \times 10^{-4} \pm 1.3 \times 10^{-5}$	92.9	
Inorganic – Zn	1.4×10^{-2}	$1.5 \times 10^{-2} \pm 3.3 \times 10^{-4}$	105.0	



rose. While the difference in color may be present due to deviations in the non-metal constituents (*e.g.*, amino acids), it is reported that high levels of iron have been observed to change the color of media to a darker yellow/orange color.^{51,52} Differences in the metal concentration and/or speciation should be discernible *via* the developed method, and so 50 μ L aliquots of each bottle were run through the procedure in triplicate.

Presented in Table 5 are the determined metal concentrations and speciation based on the calibration functions described relative to Table 4. It is expected that all Mn, Fe, Cu, and Zn would be added and remain as inorganic species whereas Co is expected to exist as a ligated species. Based on the determinations, there are clear deviations in the concentrations and speciation of the added metals in the media. The determined percentage difference from the formula values are given for each case. Uniformly, the Mn content was determined to be less than the formula values, while each of the other metals (save Zn in bottle 3), are over the target levels. As discussed before, a change to a yellow/orange color is typically associated with increased Fe levels,^{51,52} however that is not seen here. The most dramatic deviation was in fact concentration of Cu in bottle 2; $>300\times$ the target value. As can be seen for the $^{63}\text{Cu}^+$ traces of Fig. 5, the increase concentration of Cu is in the form of inorganic Cu, rather than an organometallic compound(s). Clearly, a proposed case of Fe contamination is not supported. While this method cannot attribute the change in color of the media solely to the Cu content, it does provide ready metal content feedback which could be invaluable in assessing the source of the contamination. In general, though, the developed methodology provides rapid characterization of the metal content in the media as a survey or quality control element.

3.5 Case study 2: degradation of media components as a function shelf life

As pointed out in previous discussion, uniquely among the metals, the Co content to the AMBIC 1.1 media is added in the form of cobalamin (VB₁₂). In humans, VB₁₂ plays a key role in red blood cell formation and metabolism,^{53–55} and so is likely relevant in the mammalian CHO cell processes and thus

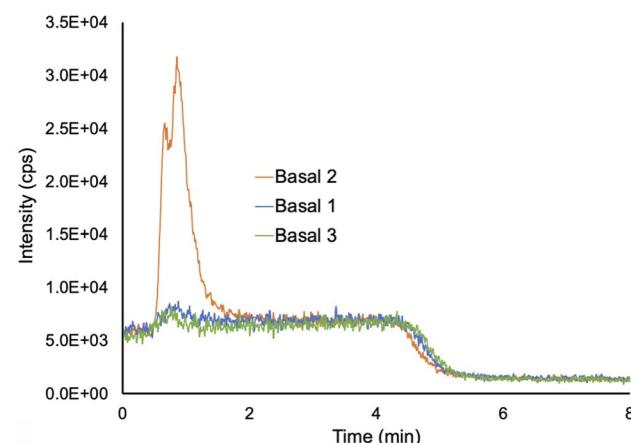


Fig. 5 C-CP fiber separation and ICP-MS traces for ^{63}Cu for the three AMBIC 1.1 CCM bottles.

a logical form to add to the CCM matrix. As shown in the chromatogram of Fig. 2, and in the quantitative analyses of Tables 4 and 5, the VB₁₂ added to the test solutions begins to dissociate on time scales of hours. It must be admitted that the

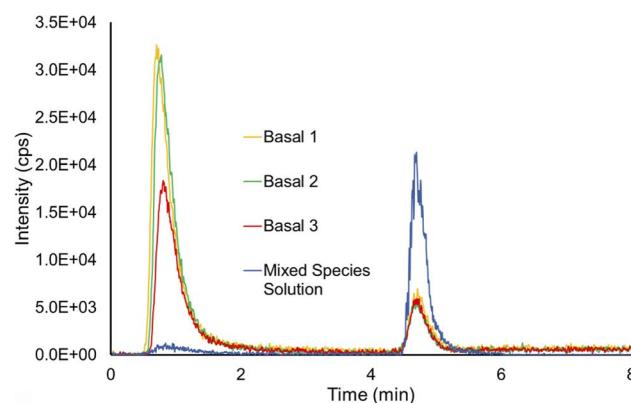


Fig. 6 C-CP fiber separation and ICP-MS response for ^{59}Co for the three AMBIC 1.1 CCM bottles and that for a freshly prepared VB₁₂ solution.

Table 5 Determined values of metal species sampled from 3 lots of AMBIC 1.1 basal media following HPLC-ICP-MS processing. Percentage difference values are based against published formula. 0-Value refers to elemental response occurring below that species' LOD

Sample bottle	Species	^{55}Mn	^{57}Fe	^{59}Co	^{63}Cu	^{64}Zn
Basal 1	Inorganic	4.1×10^{-6}	1.6×10^{-1}	3.0×10^{-3}	4.5×10^{-4}	1.7×10^{-2}
	Ligated	0	0	1.6×10^{-3}	0	0
	Total	4.1×10^{-6}	1.6×10^{-1}	4.6×10^{-3}	4.5×10^{-4}	1.7×10^{-2}
Basal 2	Percentage difference	-18.1	+21.7	+52.9	+65.4	+21.2
	Inorganic	4.4×10^{-6}	1.6×10^{-1}	2.2×10^{-3}	9.4×10^{-3}	1.7×10^{-2}
	Ligated	0	0	2.1×10^{-3}	0	0
Basal 3	Total	4.4×10^{-6}	1.6×10^{-1}	4.3×10^{-3}	9.4×10^{-3}	1.7×10^{-2}
	Percentage difference	-12.0	+17.3	+44.8	+338.7	+22.8
	Inorganic	3.0×10^{-6}	1.8×10^{-1}	1.7×10^{-3}	5.8×10^{-4}	8.0×10^{-3}
	Ligated	0	0	2.2×10^{-3}	0	0
	Total	3.0×10^{-6}	1.8×10^{-1}	3.9×10^{-3}	5.8×10^{-4}	8.0×10^{-3}
	Percentage difference	-40.5	+32.6	+28.7	+114.2	-43.5



commercial-sourced VB_{12} may itself contain free Co. Fig. 6 is composed on temporal overlays of the Co content in AMBIC 1.1 media samples Basal 1–3 (shown in Fig. 4), along with a freshly prepared VB_{12} solution whose concentration is at the target formula value. Clearly seen, while the freshly prepared sample shows $\sim 10\%$ inorganic content, the actual CCM samples show appreciable levels of degradation (assuming all Co comes from VB_{12}). As presented in Table 5, the inorganic fractions of the basal media range from 43–65%, a clear departure from what was the intended compositions. These media bottles had been stored in a dark walk-in refrigerator at a temperature of $\sim 5\text{ }^\circ\text{C}$ for approximately 6 months, a time frame not unusual for such materials. These deviations from the input values of intact VB_{12} have not been noted in the literature, as such interrogations likely have not been performed. As such, it remains unknown if those departures from the intended inputs are consequential or not, or if they occur as a general rule.

4. Conclusions

The content and chemical stability of CCM is an essential part of the production of biotherapeutics, such as mAbs, to ensure reproducibility and quality of the manufactured product. Variations in CCM metal composition and speciation have been observed across produced batches. It is postulated that these deviations may result in an ineffective media or at least variability in the product's critical quality attributes. Thus, a method of speciation and quantification is needed to provide insights on how changes in the concentration and chemical forms of metals in CCM can affect its efficacy. Developed here is a sensitive, quantitative, in-line speciation and detection method using an HPLC equipped with a polypropylene C-CP fiber column that is coupled to the Solation ICP-MS for the speciation and quantification of metals in CCM. As ICP-MS ionization is typically hindered by organic matrices, as used for the speciation, a simple apparatus utilized a flow splitter and *T*-fitting to dilute the chromatographic eluates to a tolerable organic content level (8% ACN). Initial testing of response curves demonstrated the ability of the ICP-MS to ionize and detect Mn, Fe, Co, Cu, and Zn in a matrix of a 1:10 dilution of 80% ACN + 0.1% TFA with no significant difference observed in the sensitivity, LODs (single pg mL^{-1}), LOQs, linearity, or background. Utilizing a 1:10 flow splitter and *T*-fitting, the HPLC was successfully integrated to the Solation ICP-MS, resulting in a quantitative and linear response curve over a wide dynamic range. Inorganic and ligated species were successfully separated using the reversed-phase C-CP fiber column platform with percentage recoveries ranging from 92.9 to 105.0%.

Two case studies were presented to illustrate the general utility of the methodology. In the first case, chemical contamination was suggested based on the difference in color between three bottles of basal media, assumed to have the same metal composition. While Fe was anticipated to be the culprit, Cu levels were found at $>300\times$ higher levels than the formula concentration in the second basal media bottle. While greater effort is required to discern the underlying reasoning for the

color difference and any differences in media performance, the method readily identifies this pronounced deviation from expectations. The second case study showcased the methods ability to provide evidence to the changes of metal speciation as a function shelf life time. Here VB_{12} was seen to dissociate to 43–65% inorganic deviation after 6 months, while being sheltered from light in a refrigerator. This differed greatly to a few hours old solution of VB_{12} that only saw a 10.4% inorganic Co dissociate from the vitamin.

The simple method developed here will enable future studies as to the effects that metal speciation have on cellular uptake of metals and cellular growth. Taken a step further, use of isotopic tracing of different chemical forms of a given metal could provide vital insights into preferential uptake base on speciation. It should be pointed out that the general approach can be implemented with other forms of reversed-phase chromatography columns or ICP-OES if sufficiently sensitive for the application at hand. Ultimately, this in-line separation and detection method and apparatus could be implemented across a variety of industries and research settings to address a wide variety of contamination and inconsistency issues related to metal content and speciation.

Author contributions

Cameron J. Stouffer: methodology, data curation, visualization, writing – original draft preparation; Sarah K. Wysor: methodology; R. Kenneth Marcus: conceptualization, supervision, writing – reviewing and editing.

Conflicts of interest

The authors have no conflicts of interest to declare.

Acknowledgements

Financial and instrumentation development support from Advion Corporation (Ithaca, NY) and Elemental Scientific Inc. (Omaha, NE), are gratefully acknowledged. Financial support from the Advanced Mammalian Biomanufacturing Innovation Center (AMBIC), a National Science Foundation IUCRC (grant no. EEC-2100442), is also gratefully acknowledged.

References

- 1 F. Li, N. Vijayasankaran, A. Shen, R. Kiss and A. Amanullah, Cell culture processes for monoclonal antibody production, *mAbs*, 2010, **2**(5), 466–479.
- 2 F. Torkashvand and B. Vaziri, Main Quality Attributes of Monoclonal Antibodies and Effect of Cell Culture Components, *Iran. Biomed. J.*, 2017, **21**(3), 131–141.
- 3 M. Ivarsson, T. K. Villiger, M. Morbidelli and M. Soos, Evaluating the impact of cell culture process parameters on monoclonal antibody N-glycosylation, *J. Biotechnol.*, 2014, **188**, 88–96.
- 4 B. Figueiroa Jr, E. Ailor, D. Osborne, J. M. Hardwick, M. Reff and M. J. Betenbaugh, Enhanced cell culture performance



using inducible anti-apoptotic genes E1B-19K and Aven in the production of a monoclonal antibody with Chinese hamster ovary cells, *Biotechnol. Bioeng.*, 2007, **97**(4), 877–892.

5 B. Horvath, M. Mun and M. W. Laird, Characterization of a Monoclonal Antibody Cell Culture Production Process Using a Quality by Design Approach, *Mol. Biotechnol.*, 2010, **45**(3), 203–206.

6 R. J. Graham, H. Bhatia and S. Yoon, Consequences of trace metal variability and supplementation on Chinese hamster ovary (CHO) cell culture performance: A review of key mechanisms and considerations, *Biotechnol. Bioeng.*, 2019, **116**(12), 3446–3456.

7 N. Trunfio, H. Lee, J. Starkey, C. Agarabi, J. Liu and S. Yoon, Characterization of mammalian cell culture raw materials by combining spectroscopy and chemometrics, *Biotechnol. Prog.*, 2017, **33**(4), 1127–1138.

8 N. Trunfio, H. Lee, J. Starkey, C. Agarabi, J. Liu and S. Yoon, Characterization of mammalian cell culture raw materials by combining spectroscopy and chemometrics, *Biotechnol. Prog.*, 2017, **33**(4), 1127–1138.

9 L. Huang, S. Li, W. Zhou, J. Gao, J. Yin, Z. Wang and J. Li, Cellular transport of uranium and its cytotoxicity effects on CHO-k1 cells, *Ecotoxicol. Environ. Saf.*, 2022, **246**, 114166.

10 R. J. Graham, S. A. Ketcham, A. Mohammad, E. Paregol, S. Yoon, G. Zou, T. Ju, P. J. Faustino, M. Ashraf and C. N. Madhavarao, Zinc supplementation modulates intracellular metal uptake and oxidative stress defense mechanisms in CHO cell cultures, *Biochem. Eng. J.*, 2021, **169**, 107928.

11 E. Dopp, L. M. Hartmann, A. M. Florea, U. von Recklinghausen, R. Pieper, B. Shokouhi, A. W. Rettenmeier, A. V. Hirner and G. Obe, Uptake of inorganic and organic derivatives of arsenic associated with induced cytotoxic and genotoxic effects in Chinese hamster ovary (CHO) cells, *Toxicol. Appl. Pharmacol.*, 2004, **201**(2), 156–165.

12 S. C. Galbraith, H. Bhatia, H. Liu and S. Yoon, Media formulation optimization: current and future opportunities, *Curr. Opin. Chem. Eng.*, 2018, **22**, 42–47.

13 J. E. Macdonald, J. A. Kelly and J. G. C. Veinot, Iron/Iron Oxide Nanoparticle Sequestration of Catalytic Metal Impurities from Aqueous Media and Organic Reaction Products, *Langmuir*, 2007, **23**(19), 9543–9545.

14 A. Sarkar, M. Ghosh and P. C. Sil, Nanotoxicity: Oxidative Stress Mediated Toxicity of Metal and Metal Oxide Nanoparticles, *J. Nanosci. Nanotechnol.*, 2014, **14**(1), 730–743.

15 A. Prabhu and M. Gadgil, Nickel and cobalt affect galactosylation of recombinant IgG expressed in CHO cells, *BioMetals*, 2019, **32**(1), 11–19.

16 W. Dong, P. P. Simeonova, R. Gallucci, J. Matheson, L. Flood, S. Wang, A. Hubbs and M. I. Luster, Toxic Metals Stimulate Inflammatory Cytokines in Hepatocytes through Oxidative Stress Mechanisms, *Toxicol. Appl. Pharmacol.*, 1998, **151**(2), 359–366.

17 J. Keenan, K. Horgan, M. Clynes, I. Sinkunaite, P. Ward, R. Murphy and F. O'Sullivan, Unexpected fluctuations of trace element levels in cell culture medium in vitro: caveat emptor, *In Vitro Cell. Dev. Biol.: Anim.*, 2018, **54**(8), 555–558.

18 T. Yao and Y. Asayama, Animal-cell culture media: History, characteristics, and current issues, *Reprod. Med. Biol.*, 2017, **16**(2), 99–117.

19 H. W. Lee, A. Christie, J. J. Liu and S. Yoon, Estimation of raw material performance in mammalian cell culture using near infrared spectra combined with chemometrics approaches, *Biotechnol. Prog.*, 2012, **28**(3), 824–832.

20 J. Richardson, B. Shah, P. V. Bondarenko, P. Bhebe, Z. Zhang, M. Nicklaus and M. C. Kombe, Metabolomics analysis of soy hydrolysates for the identification of productivity markers of mammalian cells for manufacturing therapeutic proteins, *Biotechnol. Prog.*, 2015, **31**(2), 522–531.

21 J. P. Mondia, F. Goh, P. A. Bryngelson, J. M. MacPhee, A. S. Ali, A. Weiskopf and M. Lanan, Using X-ray fluorescence to measure inorganics in biopharmaceutical raw materials, *Anal. Methods*, 2015, **7**(8), 3545–3550.

22 S. H. Kim and G. M. Lee, Development of serum-free medium supplemented with hydrolysates for the production of therapeutic antibodies in CHO cell cultures using design of experiments, *Appl. Microbiol. Biotechnol.*, 2009, **83**(4), 639–648.

23 F. K. Crundwell, M. S. Moats, V. Ramachandran, T. G. Robinson and W. G. Davenport, Chapter 36 – Separation of the Platinum-Group Metals from Base Metal Sulfides, and the Refining of Nickel, Copper and Cobalt, in *Extractive Metallurgy of Nickel, Cobalt and Platinum Group Metals*, ed. F. K. Crundwell, M. S. Moats, V. Ramachandran, T. G. Robinson and W. G. Davenport, Elsevier, 2011, pp. 457–488.

24 J. Pakarinen and E. Paatero, Recovery of manganese from iron containing sulfate solutions by precipitation, *Miner. Eng.*, 2011, **24**(13), 1421–1429.

25 W. Zhang and C. Y. Cheng, Manganese metallurgy review. Part II: Manganese separation and recovery from solution, *Hydrometallurgy*, 2007, **89**(3), 160–177.

26 J. M. Baust, G. C. Buehring, L. Campbell, E. Elmore, J. W. Harbell, R. W. Nims, P. Price, Y. A. Reid and F. Simione, Best practices in cell culture: an overview, *In Vitro Cell. Dev. Biol.: Anim.*, 2017, **53**(8), 669–672.

27 M. M. Gaschler and B. R. Stockwell, Lipid peroxidation in cell death, *Biochem. Biophys. Res. Commun.*, 2017, **482**(3), 419–425.

28 S. J. Dixon, K. M. Lemberg, M. R. Lamprecht, R. Skouta, E. M. Zaitsev, C. E. Gleason, D. N. Patel, A. J. Bauer, A. M. Cantley, W. S. Yang, *et al.*, Ferroptosis: an iron-dependent form of nonapoptotic cell death, *Cell*, 2012, **149**(5), 1060–1072.

29 B. Michalke, D. Willkommen and V. Venkataramani, Iron Redox Speciation Analysis Using Capillary Electrophoresis Coupled to Inductively Coupled Plasma Mass Spectrometry (CE-ICP-MS), *Front. Chem.*, 2019, **7**, 136.

30 I. H. Yuk, J. D. Zhang, M. Ebeling, M. Berrera, N. Gomez, S. Werz, C. Meiringer, Z. Shao, J. C. Swanberg, K. H. Lee,



et al., Effects of copper on CHO cells: Insights from gene expression analyses, *Biotechnol. Prog.*, 2014, **30**(2), 429–442.

31 Y. Qian, S. F. Khattak, Z. Xing, A. He, P. S. Kayne, N.-X. Qian, S.-H. Pan and Z. J. Li, Cell culture and gene transcription effects of copper sulfate on Chinese hamster ovary cells, *Biotechnol. Prog.*, 2011, **27**(4), 1190–1194.

32 N. Vijayasankaran, S. Varma, Y. Yang, M. Mun, S. Arevalo, M. Gawlitzeck, T. Swartz, A. Lim, F. Li, B. Zhang, *et al.*, Effect of cell culture medium components on color of formulated monoclonal antibody drug substance, *Biotechnol. Prog.*, 2013, **29**(5), 1270–1277.

33 A. L. Arigony, I. M. de Oliveira, M. Machado, D. L. Bordin, L. Bergter, D. Prá and J. A. Henriques, The influence of micronutrients in cell culture: a reflection on viability and genomic stability, *BioMed Res. Int.*, 2013, **2013**, 597282.

34 D. M. Templeton, F. Ariese, R. Cornelis, L. G. Danielsson, H. Muntau, H. P. Van Leeuwen and R. Lobinski, Guidelines for terms related to chemical speciation and fractionation of elements. Definitions, structural aspects, and methodological approaches (IUPAC Recommendations 2000), *Pure Appl. Chem.*, 2000, **72**(8), 1453–1470.

35 K. A. Hall, H. W. Paing and R. K. Marcus, Quantitative trace metal determinations in cell culture media using LS-APGD-MS and ICP-OES with free/bound species differentiation following polymer fiber separations, *Anal. Methods*, 2021, **13**(16), 1945–1954.

36 S. K. Wysor, K. A. Hall and R. K. Marcus, Rapid metal speciation of cell culture media using reversed-phase separations and inductively coupled plasma optical emission spectrometry, *Biotechnol. Prog.*, 2023, **39**(1), e3311.

37 L. T. Cordova, H. Dahodwala, K. S. Elliott, J. Baik, D. C. Odenewelder, D. Nmagu, B. A. Skelton, L. Uy, S. R. Klaubert, B. F. Synoground, *et al.*, Generation of reference cell lines, media, and a process platform for CHO cell biomanufacturing, *Biotechnol. Bioeng.*, 2023, **120**(3), 715–725.

38 K. M. Randunu and R. K. Marcus, Microbore polypropylene capillary channeled polymer (C-CP) fiber columns for rapid reversed-phase HPLC of proteins, *Anal. Bioanal. Chem.*, 2012, **404**(3), 721–729.

39 S. K. Wysor, K. A. Hall and R. K. Marcus, Rapid metal speciation of cell culture media using reversed-phase separations and inductively coupled plasma optical emission spectrometry, *Biotechnol. Prog.*, 2023, **39**, e3311.

40 R. C. Hutton, Application of inductively coupled plasma source mass spectrometry (ICP-MS) to the determination of trace metals in organics, *J. Anal. At. Spectrom.*, 1986, **1**(4), 259–263.

41 S. Liu, Z. Han, X. Kong, J. Zhang, Z. Lv and G. Yuan, Organic matrix effects in inductively coupled plasma mass spectrometry: a tutorial review, *Appl. Spectrosc. Rev.*, 2022, **57**(6), 461–489.

42 G. Grindlay, L. Gras, J. Mora and M. T. C. de Loos-Vollebregt, Carbon-related matrix effects in inductively coupled plasma atomic emission spectrometry, *Spectrochim. Acta, Part B*, 2008, **63**(2), 234–243.

43 D. Fliegel, C. Frei, G. Fontaine, Z. Hu, S. Gao and D. Günther, Sensitivity improvement in laser ablation inductively coupled plasma mass spectrometry achieved using a methane/argon and methanol/water/argon mixed gas plasma, *Analyst*, 2011, **136**(23), 4925–4934.

44 T. Nakazawa, D. Suzuki, H. Sakuma and N. Furuta, Comparison of signal enhancement by co-existing carbon and by co-existing bromine in inductively coupled plasma mass spectrometry, *J. Anal. At. Spectrom.*, 2014, **29**(7), 1299–1305.

45 T. Narukawa, T. Iwai and K. Chiba, An ICP index for ICP-MS determinations – new selection rules for internal standards in ICP-MS determinations and carbon enhancement effect, *J. Anal. At. Spectrom.*, 2017, **32**(8), 1547–1553.

46 B. Michalke, The coupling of LC to ICP-MS in element speciation: I. General aspects, *TrAC, Trends Anal. Chem.*, 2002, **21**(2), 142–153.

47 J. W. Olesik, Elemental analysis using ICP-OES and ICP/MS, *Anal. Chem.*, 1991, **63**(1), 12A–21A.

48 E. Chambers, D. M. Wagrowski-Diehl, Z. Lu and J. R. Mazzeo, Systematic and comprehensive strategy for reducing matrix effects in LC/MS/MS analyses, *J. Chromatogr. B*, 2007, **852**(1), 22–34.

49 A. Y. Leykin and P. V. Yakimovich, Systems for the suppression of spectral interferences for inductively coupled plasma mass-spectrometry, *J. Anal. Chem.*, 2012, **67**(8), 677–686.

50 R. Bonnett, The Chemistry of the Vitamin B12 Group, *Chem. Rev.*, 1963, **63**(6), 573–605.

51 W. Piasecki, K. Szymanek and R. Charmas, Fe²⁺ adsorption on iron oxide: the importance of the redox potential of the adsorption system, *Adsorption*, 2019, **25**(3), 613–619.

52 C. H. Weiss, C. Merkel and A. Zimmer, Impact of iron raw materials and their impurities on CHO metabolism and recombinant protein product quality, *Biotechnol. Prog.*, 2021, **37**(4), e3148.

53 M. F. Romine, D. A. Rodionov, Y. Maezato, L. N. Anderson, P. Nandhikonda, I. A. Rodionova, A. Carre, X. Li, C. Xu, T. R. Clauss, *et al.*, Elucidation of roles for vitamin B(12) in regulation of folate, ubiquinone, and methionine metabolism, *Proc. Natl. Acad. Sci. U. S. A.*, 2017, **114**(7), e1205–e1214.

54 D. Osman, A. Cooke, T. R. Young, E. Deery, N. J. Robinson and M. J. Warren, The requirement for cobalt in vitamin B(12): A paradigm for protein metalation, *Biochim. Biophys. Acta, Mol. Cell Res.*, 2021, **1868**(1), 118896.

55 F. O'Leary and S. Samman, Vitamin B12 in health and disease, *Nutrients*, 2010, **2**(3), 299–316.

